Cell Reports
Article

Genetics of Follicular Lymphoma Transformation

Laura Pasqualucci,[1,2,3,*] Hossein Khiabanian,[4] Marco Fangazio,[1] Mansi Vasishtha,[1] Monica Messina,[1] Antony B. Holmes,[1] Peter Ouillette,[5] Vladimir Trifonov,[4] Davide Rossi,[6] Fabrizio Tabbò,[7] Maurilio Ponzoni,[8] Amy Chadburn,[9] Vundavalli V. Murty,[1,2,3] Govind Bhagat,[2,3] Gianluca Gaidano,[6] Giorgio Inghirami,[7] Sami N. Malek,[5] Raul Rabadan,[4] and Riccardo Dalla-Favera[1,2,3,10,11,*]

[1]Institute for Cancer Genetics, Columbia University, New York, NY 10032, USA
[2]Herbert Irving Comprehensive Cancer Center, Columbia University, New York, NY 10032, USA
[3]Department of Pathology & Cell Biology, Columbia University, New York, NY 10032, USA
[4]Department of Biomedical Informatics and Center for Computational Biology and Bioinformatics, Columbia University, New York, NY 10032, USA
[5]Department of Internal Medicine, Division of Hematology and Oncology, University of Michigan, Ann Arbor, MI 48109, USA
[6]Division of Hematology, Department of Translational Medicine, Amedeo Avogadro University of Eastern Piedmont, Novara 28100, Italy
[7]Department of Molecular Biotechnology and Health Science, Center for Experimental Research and Medical Studies (CeRMS), University of Torino, Torino 10126, Italy
[8]Pathology and Lymphoid Malignancies Units, San Raffaele Scientific Institute, Milan 20132, Italy
[9]Department of Pathology, Feinberg School of Medicine, Northwestern University, Chicago, IL 60611, USA
[10]Department of Genetics & Development, Columbia University, New York, NY 10032, USA
[11]Department of Microbiology & Immunology, Columbia University, New York, NY 10032, USA
*Correspondence: lp171@columbia.edu (L.P.), rd10@columbia.edu (R.D.-F.)
http://dx.doi.org/10.1016/j.celrep.2013.12.027

SUMMARY

Follicular lymphoma (FL) is an indolent disease, but 30%–40% of cases undergo histologic transformation to an aggressive malignancy, typically represented by diffuse large B cell lymphoma (DLBCL). The pathogenesis of this process remains largely unknown. Using whole-exome sequencing and copy-number analysis, we show here that the dominant clone of FL and transformed FL (tFL) arise by divergent evolution from a common mutated precursor through the acquisition of distinct genetic events. Mutations in epigenetic modifiers and antiapoptotic genes are introduced early in the common precursor, whereas tFL is specifically associated with alterations deregulating cell-cycle progression and DNA damage responses (*CDKN2A/B*, *MYC*, and *TP53*) as well as aberrant somatic hypermutation. The genomic profile of tFL shares similarities with that of germinal center B cell-type de novo DLBCL but also displays unique combinations of altered genes with diagnostic and therapeutic implications.

INTRODUCTION

Follicular lymphoma (FL) is the second most common type of B cell non-Hodgkin lymphoma, comprising ~25% of all new diagnoses (Swerdlow et al., 2008) (http://seer.cancer.gov/statistics/). Although initially indolent and responsive to a variety of treatments, this disease remains largely incurable (Kridel et al., 2012). One particularly compelling problem in the clinical history of FL is its histologic transformation to a more aggressive malignancy, typically represented by a diffuse large B cell lymphoma (DLBCL) (Montoto and Fitzgibbon, 2011). FL transformation has been reported to occur in 16% to 70% of patients over time, with a consensus rate of 3% per year, and is associated with a mean survival posttransformation of less than 2 years (Montoto and Fitzgibbon, 2011). Thus, there is a strong need for an increased understanding of both the dynamics of tumor clonal evolution and the mechanisms that are responsible for transformation, which may in turn be translated into more effective therapies.

Although the process of transformation to DLBCL was originally described several decades ago, few studies have specifically addressed this question in longitudinal series with documented clonal relationship between the two phases (Lossos and Gascoyne, 2011). Current knowledge of the biology of transformation suggests the involvement of heterogeneous genetic, epigenetic, and microenvironment-dependent factors, most notably mutations of *TP53* (Lo Coco et al., 1993; Sander et al., 1993), genetic and/or epigenetic inactivation of the *CDKN2A*/p16 tumor suppressor gene (Pinyol et al., 1998), translocations deregulating the *BCL6* proto-oncogene (Akasaka et al., 2003), alterations involving chromosome 1p36 (Martinez-Climent et al., 2003), and changes in *MYC* expression (Lossos et al., 2002). Additionally, analysis of selected genes in few cases revealed an association between progression to DLBCL and aberrant somatic hypermutation (ASHM) (Rossi et al., 2006), a mechanism of genetic instability resulting from the abnormal functioning of the physiologic somatic hypermutation (SHM) process that operates in germinal center (GC) B cells (Pasqualucci et al., 2001). However, these findings were based on small number of cases and a candidate gene approach as opposed to an

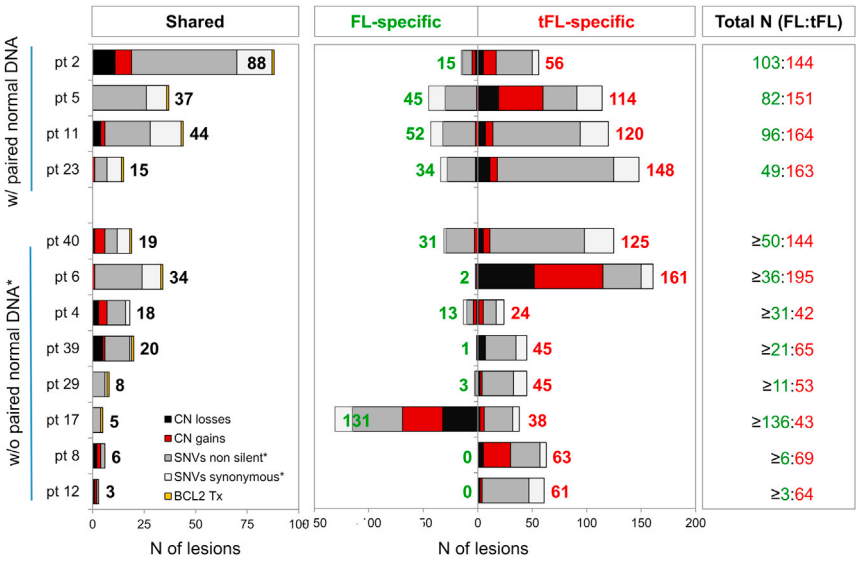

Figure 1. FL and tFL Display Shared and Unique Genomic Aberrations

Overall load of genetic lesions identified by WES and CN analysis in the dominant clone of the 12 discovery cases. Color codes denote distinct types of aberrations (Tx, translocation). *In cases lacking matched normal DNA, shared SNVs are limited to those affecting 52 selected genes with well-established roles in lymphomagenesis (see the Experimental Procedures); thus, the total number of genetic lesions in these patients (right column) most likely represents an underestimate. FL-specific SNVs that could be due to genomic loss or cnLOH of the same region in the tFL phase were excluded.

unbiased, genome-wide analysis. Thus, the biological mechanisms that are responsible for the lethal event of FL transformation remain incompletely understood.

The present study was aimed at examining the history of clonal evolution during FL transformation to DLBCL and comprehensively identifying molecular determinants that underlie this process.

RESULTS

Divergent Evolution of FL and tFL from a Common Mutated Precursor

To investigate whether transformation of FL evolves as a linear process (i.e., through the emergence of an aggressive subclone from the initial dominant FL population) or derives from the divergent evolution of an ancestral common precursor cell (CPC) that acquired distinct mutations to become a FL or a transformed FL (tFL), we integrated massively parallel whole-exome sequencing (WES) and genome-wide high-resolution SNP array analysis in a "discovery panel" of sequential FL and tFL biopsies obtained from 12 patients, including four with available matched normal DNA (Tables S1 and S2 and Figure S1). In all cases, investigation of the rearranged immunoglobulin (Ig) genes by Sanger sequencing and/or SNP array analysis confirmed the clonal relationship between the two phases, whereas the inferred copy-number value at the segment of deletional recombination within the Ig loci was used to quantify the percentage of tumor cells in the biopsy (Bergsagel and Kuehl, 2013), allowing to normalize the data for clonal representation (Table S1). Fluorescence in situ hybridization (FISH) analysis was used to assess the presence of chromosomal translocations affecting *BCL2*, *MYC*, and *BCL6*.

We extrapolated the evolutionary history of transformation by defining genomic alterations that are present in the dominant clone of both pre- and posttransformation specimens ("shared lesions") and contrasting them to those that are present exclusively in the FL or tFL biopsy ("phase-specific lesions"). This analysis allows to discriminate between a linear, sequential model, wherein the tFL dominant clone will maintain all lesions present in the FL dominant clone, along with additional tFL-acquired alterations, and a divergent evolution model, which postulates the existence of lesions that are unique to the dominant clone of the FL or the tFL in addition to the set of shared alterations (Experimental Procedures and Figure S1).

Overall, we found 52 clonally represented, shared copy-number aberrations (CNAs; average, 4.3 per sample; range, 0 to 19 per sample) and 234 shared single-nucleotide variants (SNVs), including silent and nonsilent mutations (average, 38.5 per sample in the four patients with matched normal DNA; in the remaining eight pairs, shared SNVs were only considered if they affected 52 genes that have been previously validated as functional targets of somatic mutations in lymphoid malignancies, because of the exceedingly high number of variants that are predicted in the absence of matched normal DNA, most likely reflecting private SNPs not reported in public databases; see the Experimental Procedures). The presence of shared genetic alterations was documented in all sample pairs analyzed, confirming the original clonal relationship between the FL and tFL sample (Figure 1, left).

In addition to shared lesions, all tFL cases harbored unique mutations and CNAs that were not present in the major FL clone at diagnosis, indicating acquisition during the transformation process or selection of a minor subclone, the size of which was below the detection threshold of the methodologies used. The number of tFL-specific lesions (n = 709 SNVs and 291 CNAs, including 119 losses and 172 gains) was widely heterogeneous across different patients, ranging from 24 to 161 per case (average, 83 per sample) (Figure 1, right; see also Figure S2A and Table S3). Importantly, unique, clonally represented events were also detected in 10 of 12 baseline FL biopsies (n = 327, including 229 SNVs and 98 CNAs; Figure 1, middle, and Figure S2A). The presence of FL-specific lesions was not due to CN loss or copy-neutral loss of heterozygosity (cnLOH) affecting the same region in the sequential tFL biopsy, as documented by both SNP array and WES analysis. Thus, these events had been acquired independently by the dominant FL clone, consistent with divergent evolution.

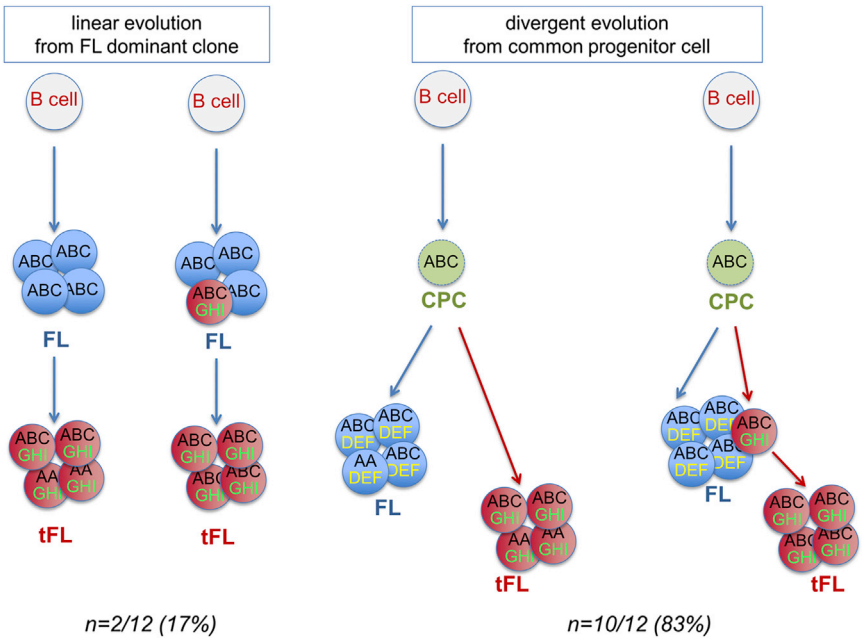

Figure 2. FL and tFL Arise through Divergent Evolution in Most Patients

Inferred models of clonal evolution during FL transformation. The original B cell clone is on top; blue and red circles depict the FL and tFL clones, respectively, whereas green, dotted circles represent the postulated common mutated precursor cell (CPC). In the linear model (2 of 12 patients analyzed), the tFL dominant clone originates directly from the FL dominant clone after the acquisition of additional mutations. In the divergent model (10 of 12 patients analyzed), the FL and tFL dominant clones derive from a CPC through the independent acquisition of distinct mutations. In both scenarios, the tFL dominant clone may be present as a minor subclone already at the time of the FL biopsy (not addressed in this study). ABC, mutations shared between FL and tFL; DEF, mutations unique to the FL dominant clone; GHI, mutations unique to the tFL dominant clone.

Evidence of nonlinear evolution was also observed at the individual gene level. As an example, both FL and tFL of patient #23 harbored biallelic *MLL2* mutations in the dominant clone, but only one of the two events (S286fs) was shared between the pre- and posttransformation biopsy, consistent with its presence in the common ancestor clone, whereas distinct mutations were detected in the second allele of the FL (R2687*) and tFL (R280_splice) specimen, indicating that they had been acquired independently by the ancestor clone during evolution to these two diseases (Figures S2B–S2D).

Overall, 10 of 12 patients analyzed (83.3%; 95% confidence interval [CI], 55% to 95%) showed a mutation pattern suggestive of divergent evolution, indicating that this is the predominant mode in the history of FL transformation (Figure 2). The remaining two patients (#8 and #12) did not harbor FL-specific events; furthermore, a significant proportion of tFL-specific lesions (13 of 63 in patient #8 and 34 of 61 in patient #12) could be detected at low frequencies (4% to 15%) in the FL specimen, suggesting that the tFL arose from a minor subclone within the dominant FL population, which subsequently acquired additional mutations in a linear evolution pattern (Figure 2 and Table S3).

With one exception (patient #17), the number of events acquired by the tFL dominant clone (including CNAs and SNVs) was significantly higher than that acquired by the FL dominant clone, ranging from >50-fold in case #6 to 2-fold in case #11 ($p < 0.005$) and underscoring the genomic complexity of the tFL genome (Figures 1 and S3A). Notably, at least one of these ten patients did not receive any treatment between the original FL diagnosis and transformation, indicating that the higher mutation load of tFL does not simply reflect the consequence of the mutagenic effect or the selective pressure of chemotherapy. In at least two patients, several chromosomes displayed convoluted intrachromosomal rearrangements due to alternating gains and losses of genomic material, frequently accounting for over ten switches per chromosome (Figure S3B and Table S4). Although the sequencing approach adopted in our study (WES, as opposed to whole-genome sequencing) prevents from distinguishing true chromothripsis from localized lesions that occurred progressively (Korbel and Campbell, 2013), these data highlight a remarkable genomic instability in tFL cases in comparison to both FL and other lymphoid malignancies (Fabbri et al., 2011; Mullighan et al., 2007; Rossi et al., 2012).

Collectively, these findings support a divergent evolution model in a significant proportion of patients undergoing transformation, whereby FL and tFL arise from a common mutated ancestor through the independent acquisition of distinct genetic lesions.

Recurrent Genetic Lesions

In order to identify lesions potentially relevant for transformation among the large number of candidates that emerged from the analysis of the discovery panel (710 unique genes, including those targeted by nonsilent SNVs, small indels, and/or CNAs if they were within minimal common regions involving a maximum of three loci), we extended the WES and SNP array analysis to 27 additional tFL cases (screening panel; combined, 39 tFL cases). Then, these data were interrogated for the presence of recurrent alterations, a common readout for functionally relevant genes, and by three independent analytical methods for the identification of key targets of functional genomic alterations: (1) MutComFocal, a recently developed computational algorithm that isolates candidate cancer genes from high throughput CN and SNV data (Trifonov et al., 2013a), (2) MutSigCV, a tool that analyzes SNV data in order to identify genes mutated more often than expected by chance (Lawrence et al., 2013), and (3) GISTIC, a computational approach identifying significant targets of somatic CNAs.

Figure 3 illustrates the overall proportion of tFL cases harboring genetic lesions in genes altered at $\geq$10% frequency and recognized as functionally relevant targets by at least one

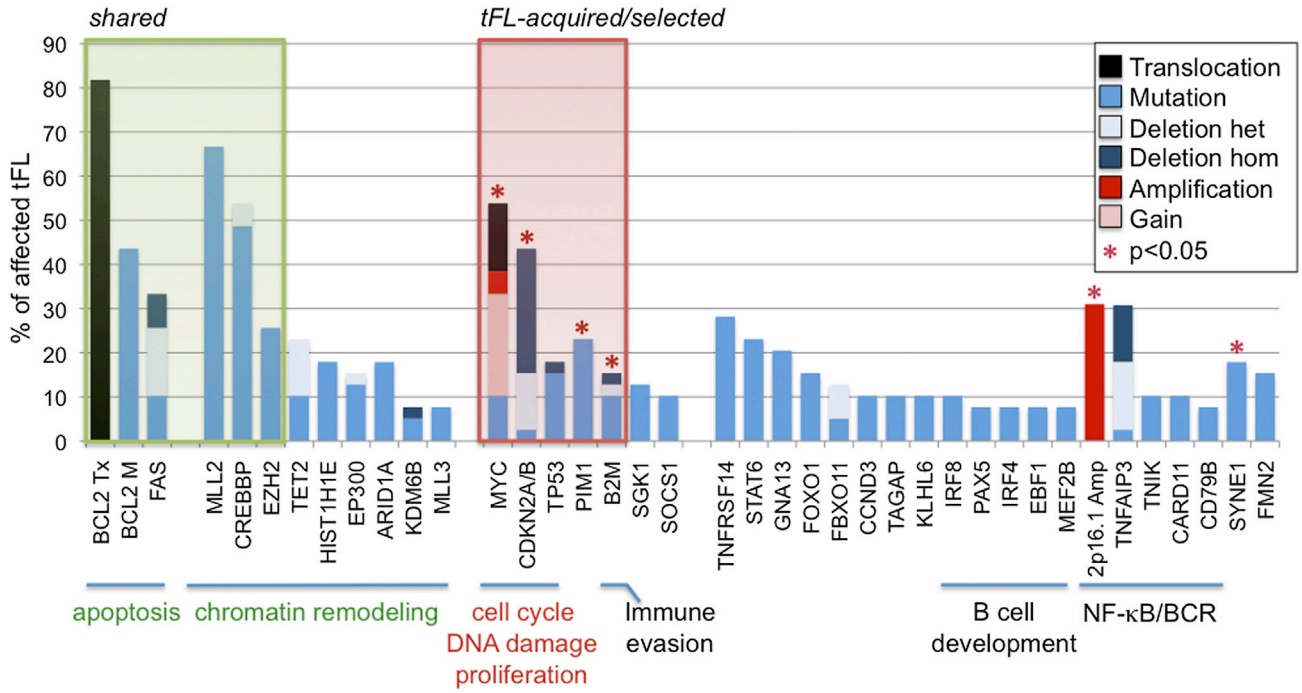

Figure 3. Recurrently Mutated Genes in tFL

Proportion of tFL cases (n = 39) carrying genetic lesions (SNVs and CNAs) in genes altered at ≥10% frequency and deemed significant by one of three independent algorithms (see the Supplemental Information and Table S5); additional genes of functional relevance in the same pathways are also shown. Deletions and gains were only computed if defining MCRs of aberration encompassing a maximum of three genes. Green shade highlights alterations consistently shared between the FL and tFL sample, and red shade identifies alterations enriched in tFL (*p < 0.05 when comparing tFL frequency versus unselected FL frequency; note that *TP53* was considered as a tFL-specific target despite its borderline p value because it was invariably unmutated in the diagnostic FL sample of all three informative tFL cases and because of the broad literature data. The remaining genes did not appear to be phase-specific or could not be unequivocally assigned to a given category because of the relatively small numbers (for the full list of SNVs found in >5% of tFL cases, see Table S7).

of the three independent approaches, with few additional genes of functional annotation within the same pathway (see Figures S4–S6 and Table S5 for the full list of genes found mutated in ≥ 10% of cases; see also Table S6). Genes are grouped into biological categories and annotated in order to indicate whether alterations were also found in the diagnostic FL biopsy (available in 24 of the 39 cases) or predominantly acquired or selected at transformation. Collectively, these aberrations point to a number of biological programs and signaling pathways that are either dysregulated early in the putative FL and tFL precursor cell (i.e., "shared" lesions) or selected during transformation ("tFL-acquired" lesions).

Genetic Lesions Shared by FL and tFL

The most commonly affected genes in both FL and tFL were those encoding for histone modification enzymes, including methyltransferases and acetyltransferases (36 of 39 cases [92.3%]). In line with previous findings in unselected FL (Morin et al., 2010; Morin et al., 2011; Pasqualucci et al., 2011a; Pasqualucci et al., 2011b), the H3K4 trimethyltransferase *MLL2* was mutated in 26 of 39 tFL cases (66.7%) with 36 truncating events and nine missense mutations (Figures 3, S4, and S6 and Table S7). These lesions were already present at FL diagnosis in all but one patient and were never lost at transformation, consistent with an early acquisition by the CPC. The activity of the MLL2-containing complex was also impaired by mutually exclusive alterations of *KDM6B*, encoding for an H3K4 histone demethylase interacting with MLL2 (n = 3 of 39 cases, including two SNVs and one homozygous deletion) and *MLL3* (n = 3 of 39 cases; Figures S4 and S6 and Table S7). Additionally, one-fourth of tFL cases (n = 10 of 39 [25.6%]) harbored *EZH2* gain-of-function mutations that almost invariably replace the hotspot tyrosine residue Y641 within the protein SET domain (n = 9 of 10; Table S7). *EZH2* mutations have been reported in 7% unselected FL cases and 22% de novo GCB-DLBCL (Morin et al., 2010; Morin et al., 2011), where they increase H3K27 levels through altered substrate specificity.

Another class of chromatin modifiers was represented by the acetyltransferases *CREBBP* (n = 21 of 39 patients [53.8%]; 19 point mutations and two focal deletions) and *EP300* (6 of 39 cases [15.4%], of which five mutated and one deleted; Figures 3, S4, and S6). In both genes, the mutation pattern was highly reminiscent of what has been reported in unselected FL and de novo DLBCL with respect to the inactivating nature of the lesions, the evidence of mutational hotspots (R1446 in five patients, F1484 in two patients, Y1503 in two patients, and ΔS1680 in three patients; Table S7), and the predominantly monoallelic distribution (19 of 21 affected cases), indicating a haploinsufficient tumor suppressor role (Pasqualucci et al., 2011a).

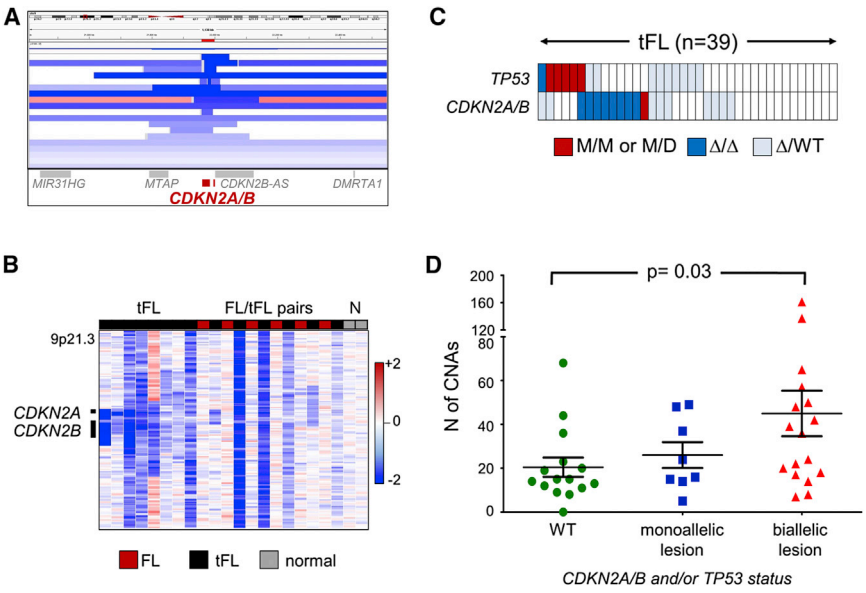

Figure 4. Biallelic Loss of *CDKN2A/B* Is Specifically Acquired during Transformation

(A) Segmentation data from 18 DLBCL samples harboring *CDKN2A/B* deletions, visualized with the Integrative Genomics Viewer (http://www.broadinstitute.org/igv). Each track represents one sample, wherein white denotes a normal (diploid) copy number, blue indicates a region of copy-number loss, and red corresponds to a region of copy-number gain. The inferred copy number and the corresponding color intensity may vary across samples because of the presence of nontumor cells infiltrating the biopsy. Individual genes in the region are aligned in the bottom panel, and the area defined by the red bar at the top corresponds to the *CDKN2A/B* locus.

(B) dChipSNP heatmap showing median-smoothed log2 CN ratio in 14 tFL biopsies harboring *CDKN2A/B* deletions, including six with matched FL biopsies and two control DNAs (N). A vertical black bar indicates the location of the *CDKN2A/B* loci.

(C) Relative distribution of biallelic lesions affecting *CDKN2A/B* and *TP53*. Columns correspond to individual patients, and the genomic status of the two genes is color-coded as indicated.

(D) Samples carrying biallelic alterations of *CDKN2A/B* and/or *TP53* are characterized by a significantly higher number of CN aberrations (Mann-Whitney U test, p = 0.03).

Programmed cell death was the second largest program dysregulated in both FL and tFL and, thus, presumably in the common ancestor clone. In addition to *BCL2* translocations, detected in 27 of 33 tFL (81.8%) and invariably shared between the two phases (n = 18 informative pairs), all t(14;18)-positive cases harbored multiple somatic point mutations within the ~2 kb region downstream of the *BCL2* transcription initiation sites (Figure 3 and S4 and Table S7), reflecting the activity of the AID-dependent SHM process driven by the juxtaposed Ig enhancer (Lohr et al., 2012; Saito et al., 2009).

The *FAS* gene was disrupted in 13 of 39 tFL cases (33.3%) because of inactivating mutations (n = 4 of 39 [10.2%]) and genomic deletions (n = 9 of 39 [23.1%], including two focal homozygous events; Figures 3 and S4). In the three affected patients with available pre- and posttransformation biopsy, these lesions were always detectable at FL diagnosis, suggesting their presence in the putative CPC (Table S7). Interestingly, none of the 23 unselected FL exomes harbored *FAS* mutations, giving rise to the possibility that these lesions represent an early marker for transformation. *FAS* encodes for a receptor protein that acts as a major mediator of apoptosis in GCB cells carrying low-affinity and self-reactive antigen receptors (van Eijk et al., 2001). With the exception of one amino acid substitution removing the initiating methionine (M1T), all *FAS* mutations (Y232*, P217_splice, and D317V) cluster in exons 7 to 9, which encode for the protein intracytoplasmic tail (Table S7). This domain is required for the assembly of the death-inducing signaling complex, and its truncation will result in the functional loss of normal FAS signaling by a dominant-negative effect (Siegel et al., 2000), as documented in patients with autoimmune lymphoproliferative syndrome (Holzelova et al., 2004). A deleterious effect was also predicted for the D317V amino acid change on the basis of the PolyPhen 2 algorithm (Table S7). *FAS* was identified as a relevant target of genomic deletions by two independent algorithms, including GISTIC (Figure S5 and Table S6) and MutComFocal.

Altogether, these findings identify the disruption of pathways affecting chromatin modifier functions and resistance to apoptosis as recurrent lesions common to FL and tFL, and, thus, presumably occurring early during the initial clonal expansion of the putative precursor clone.

Genetic Lesions Specifically Associated with tFL

The most common genomic aberration specifically acquired during progression to tFL was the loss of *CDKN2A/B*, two tumor suppressor genes whose protein products (p14-ARF, p16-INK4A, and p15-INK4B) play major roles as negative regulators of cell-cycle G1 progression and as stabilizers of the tumor suppressor p53 (Sherr, 2004). Overall, 46.1% of tFL cases (n = 18 of 39) carry genomic aberrations affecting these loci, including 17 CN losses (n = 6 heterozygous and 11 homozygous; Figure 4A) and a nonsense C72* mutation combined with cnLOH (Figure S4 and Table S7). In most deleted cases (n = 10 of 17), the loss of genetic material encompassed $\leq$ 3 genes, identifying a minimal common region smaller than 10 kb and exquisitely restricted to the *CDKN2A/B* locus. Biallelic *CDKN2A/B* alterations were never present at FL diagnosis, indicating a specific role during transformation (Figure 4B).

The loss of *CDKN2A/B* may impinge on different biological programs, including DNA damage responses (via the p14-ARF/p53 pathway) and cell-cycle regulation (via the RB/p16 tumor-suppressive pathway). As expected, immunohistochemical staining for p16 expression confirmed its complete loss in the neoplastic lymphocytes of all biallelically deleted tFL cases

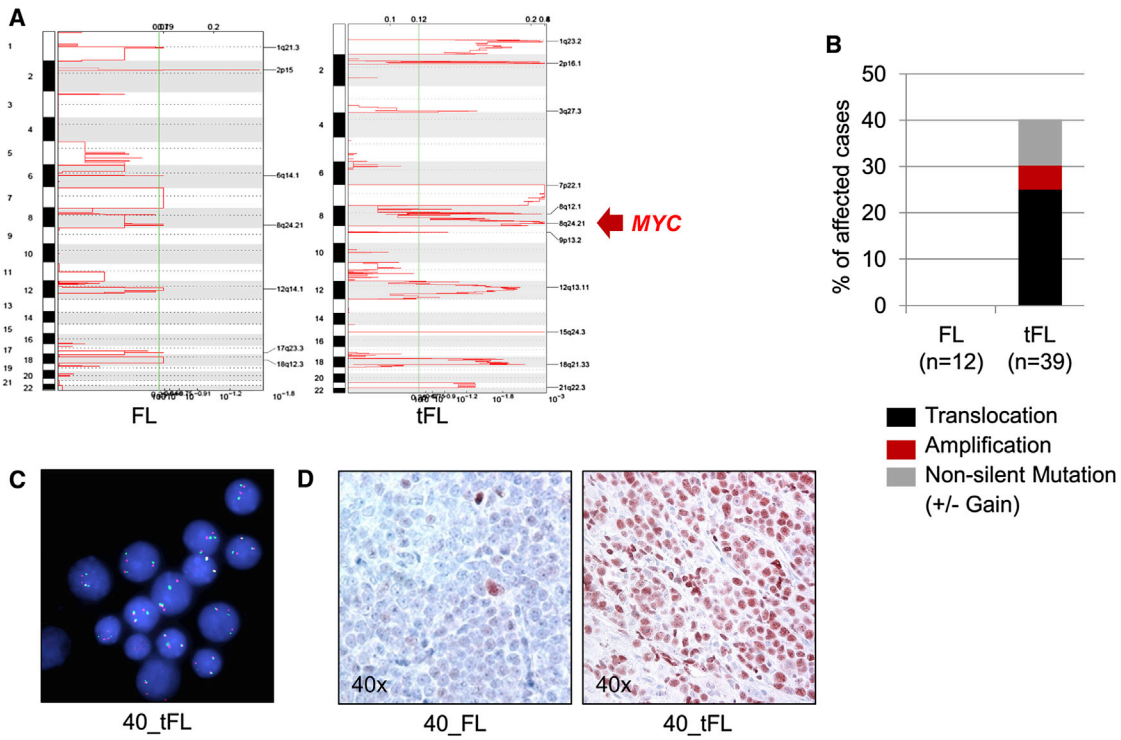

Figure 5. Recurrent Genetic Lesions of *MYC* in tFL

(A) GISTIC analysis of CN gains in FL and tFL cases (see also Figure S5).

(B) Percentage of cases carrying genetic lesions of *MYC* in FL and tFL.

(C) FISH analysis with a *MYC* break-apart probe in tFL #40.

(D) IHC analysis of *MYC* expression in the pre- and posttransformation biopsy of the same patient.

(n = 8 of 8); however, two of three monoallelically deleted cases and a significant proportion of wild-type (WT) tFL cases (n = 5 of 15 [33.3%]) were also p16-negative (data not shown), suggesting the involvement of epigenetic mechanisms of inactivation. Although the limited number of cases prevents statistical analysis, *CDKN2A/B* biallelic lesions tend to be mutually exclusive with biallelic deletions and/or mutations of *TP53*, observed in 7 of 39 tFL cases (17.9%) but absent at FL diagnosis (n = 3 informative cases; Figure 4C). These observations suggest that *CDKN2A/B* loss may contribute to FL transformation by affecting both cell-cycle regulation and p53-dependent DNA damage responses, thus promoting genomic instability. Consistent with this hypothesis, patients exhibiting dysregulation of the ARF/p53 axis via biallelic alterations of *CDKN2A/B* and/or *TP53* were characterized by a significantly higher number of CNAs in comparison to patients that harbor WT alleles (average n = 45.0 versus 20.5, Mann Whitney U test, p = 0.03; Figure 4D).

Genetic lesions deregulating *MYC*, namely chromosomal translocations (n = 6 of 24 tFL cases with available FISH data [25.0%]), copy-number gains and/or amplifications (n = 13 of 39 [33.3%]), and point mutations reflecting the activity of ASHM (Figures 5 and S4 and Table S7) were the second most common tFL-specific lesions. Although low copy-number gains could be occasionally observed in the original FL biopsy, high CN amplifications, translocations, and point mutations were either completely absent (n = 13 cases) or only detected in a minor subclone within the dominant FL population (patient #8). Deregulated *MYC* oncogenic activity may provide multiple advantages to the cancer cell through its pleiotropic function in cell growth, metabolism, and genetic instability.

Also enriched at transformation were biallelic mutations and/or deletions encompassing *B2M* (n = 5 of 39) and *CD58* (n = 2 of 39), two genes involved in the control of immune recognition by cytotoxic T lymphocytes and natural killer cells, respectively, and previously shown to be recurrently inactivated in de novo DLBCL (Challa-Malladi et al., 2011) (Figures 3 and S4 and Tables S6 and S7). *B2M* genomic aberrations were specifically acquired or selected at transformation (n = 3 informative cases) and, accordingly, *B2M* as well as *CD58* were not mutated in 23 unselected FL exomes analyzed, implicating escape from immune surveillance as a contributor to the transformation process.

Finally, multiple point mutations, small deletions, and duplications were identified in the 5′ sequences of several recognized ASHM target genes, including *PIM1*, *PAX5*, *RhoH/TTF*, *MYC*, *BCL7A*, *CIITA*, and *SOCS1* (overall, 34 of 39 cases [87.1%]; Figure 6). These lesions display typical features of AID-mediated activity (Figure S7) and, depending on the genomic configuration of the involved locus, were variably distributed in coding and/or noncoding sequences. These changes were not detected in the pretransformation biopsy, indicating that they had been

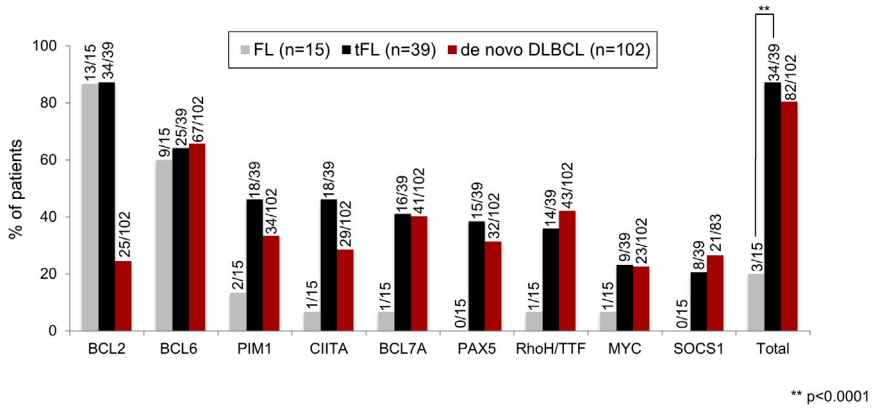

Figure 6. ASHM Is Associated with Transformation

Proportion of cases harboring mutations in known ASHM targets; the BCL6 intron 1 region, a physiologic target of SHM in GC B cells, and the BCL2 sequences, which accumulate mutations in translocated alleles under the influence of the juxtaposed *IGH* promoter, are shown as controls. The three mutated FL cases harbored one single event each.

specifically acquired or selected at transformation (Figure 6). These data point to a malfunction of SHM occurring late in the disease, although the prolonged exposure of the precursor cell to the potentially deleterious environment of the GC reaction may also favor the accumulation of lesions.

Non-Phase-Specific Lesions

A number of genetic alterations were variably observed as shared or phase-specific events, suggesting heterogeneous contributions to disease pathogenesis. Consistent with previous reports (Lossos and Gascoyne, 2011), *TNFRSF14*, encoding for a member of the TNF receptor superfamily that signals to T cells with stimulatory or inhibitory effects depending on the ligand, was disrupted in 22 of 39 tFL (56.4%) and 9 of 17 FL cases (52.9%) due to a combination of truncating mutations (n = 14, distributed in 11 tFL and 3 FL cases), genomic deletions (n = 15 tFL and 6 FL cases), and cnLOH (n = 4 tFL cases and 1 FL case; Figure S4 and Table S7). Importantly, all mutated tFL cases had lost the residual WT allele because of deletion or cnLOH. Although multiple other candidate genes are encompassed by the large heterozygous deletions affecting chromosomal region 1p36.31, this typical pattern of biallelic inactivation documented the specific involvement of *TNFRSF14* in these lesions (Figure S4).

STAT6, a DNA binding transcription factor implicated in IL4 and IL13-mediated responses, was the target of heterozygous somatic point mutations in 9 of 39 (23.1%) tFL cases. Analysis of the diagnostic FL biopsy revealed the presence of the same mutation in three of five available cases, whereas the remaining two had acquired this lesion at transformation; *STAT6* mutations were observed in unselected FL cases (1 of 23 [4.3%]), consistent with a role in both disease phases. Notably, all *STAT6* mutations cluster within the protein DNA binding domain, identifying a mutational hotspot of possible functional relevance at residue D419, which was substituted to G (four cases), H (one case), and Y (one case; Figure S4 and Table S7), as previously reported in primary mediastinal B cell lymphoma (Ritz et al., 2009).

Several genes encoding for core histones were also frequently mutated in both tFL (n = 11 of 39 [28.2%]) and FL (n = 6 of 12 [50%]) cases, *HIST1H1E* being the most common target (n = 7 of 39 tFL [17.9%], 2 of 12 FL, [16.6%], and 2 of 23 unselected FL cases [8.7%]; Tables S5 and S7). In addition, > 10% of tFL cases harbored loss-of-function (nonsense and frameshift) mutations disrupting the *ARID1A* (n = 7 of 39 [17.9%]) and *ARID1B* (n = 1 of 39 [2.6%]) genes, two components of the SWI-SNF chromatin remodeling complex, which was recently shown to take part in maintaining the pluripotency of stem cells as well as in reprogramming somatic cells (Ho et al., 2009).

Finally, a number of recurrent lesions are expected to interfere with signaling pathways that are triggered in response to engagement of the BCR or CXCR4 receptors; these include oncogenic mutations of *CARD11* and *CD79B* (4 of 39 tFL [10.3%] and 3 of 39 tFL cases [7.7%], respectively), alterations in negative and positive regulators of NF-κB (*TNFAIP3*, biallelically lost in 6 of 39 tFL cases, and TRAF2- and Nck-interacting kinase [*TNIK*], mutated in 4 of 39 cases), truncating mutations of *GNA13* (n = 8 of 39 tFL [20.5%] versus 1 of 23 unselected FL cases [4.3%]), and point mutations of *FOXO1* (n = 6 of 39 tFL [15.4%] versus 0 of 23 unselected FL cases; Tables S5 and S7); deregulation of the latter two genes may impinge on the PI3K pathway as well as RhoGTPase responses, and has been observed in de novo DLBCL (Morin et al., 2013; Trinh et al., 2013). Altogether, these results point to several signaling pathways that are recurrently dysregulated in FL and/or tFL, although their individual contribution is not specifically restricted to a discrete phase of disease pathogenesis (see the Discussion).

The Genomic Landscape of tFL Is Unique But More Related to GCB-DLBCL

In order to determine whether tFL and de novo DLBCL represent pathogenically different diseases, we compared the genomic profile of the 39 tFL cases to that of 102 de novo DLBCL cases representative of the two major molecular subtypes; i.e., GCB and activated B cell (ABC) DLBCL (Alizadeh et al., 2000). When analyzed by unsupervised hierarchical clustering with the frequency of aberrations at 34 informative targets, tFL appears to be closer to GCB- than ABC-DLBCL (see the Experimental Procedures). Common features of the two diseases include the presence of *BCL2* rearrangements, *REL* amplifications, *EZH2*, *GNA13*, and *TNFRSF14* mutations (Morin et al., 2010, 2011; Pasqualucci et al., 2011b) along with the absence of typical ABC-DLBCL-specific aberrations (*MYD88* mutations and *PRDM1* inactivation) (Mandelbaum et al., 2010; Morin et al., 2013; Ngo et al., 2011; Pasqualucci et al., 2006) (Figure 7). However, unique combinations of genetic lesions were found in tFL, which are otherwise never observed in GCB-DLBCL (e.g., biallelic

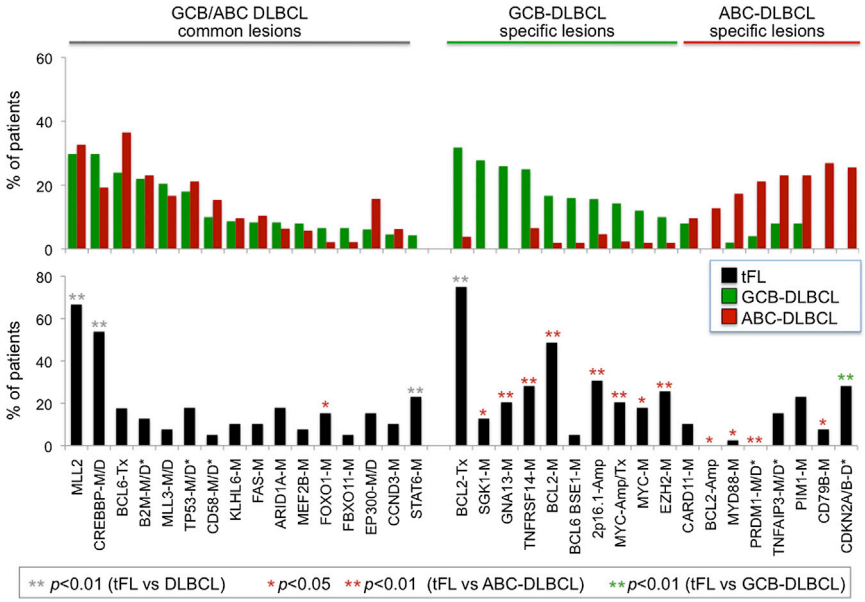

Figure 7. tFL Displays a Unique Genomic Profile that Partially Overlaps with GCB-DLBCL

Percentage of cases carrying the indicated genetic lesions in de novo DLBCL (top: green bars, GCB-DLBCL; n = 50; red bars, ABC-DLBCL; n = 52) and tFL (bottom: black bars; n = 39). Asterisks indicate statistically significant differences (one-tailed Fisher's exact test; *p < 0.05, **p < 0.01). Mutation frequencies for *SGK1* and *GNA13* are derived from Morin et al., 2011. M, mutation (missense, nonsense, frameshift, and splice-site); D, deletion; G, gain; AMP, amplification; M/D*, biallelic inactivation; Tx, translocation; BSE1, binding site in exon 1.

deletions of *CDKN2A/B*; 28.2% of tFL cases versus 0% of GCB-DLBCL, p < 0.01). Moreover, tFL tends to be enriched in alterations that are generally less frequent in de novo DLBCL, such as *STAT6* mutations (23.1% versus 2.4%), *ARID1A* mutations (17.9% versus 7.2%), and *FAS* mutations and/or deletions (33.3% versus 16.7%). Particularly, although observed in both tFL and de novo DLBCL, aberrations of *MLL2*, *CREBBP*, and *BCL2* were significantly enriched in cases derived from FL transformation in comparison to GCB-DLBCL (p = 0.02, 0.0006, and 0.0001), suggesting that at least a subset of GCB-DLBCL arises from the precursor cell postulated by the results described above. In conclusion, the genome of tFL appears more similar to GCB-DLBCL but, overall, is unique in comparison to both subtypes of de novo DLBCL.

DISCUSSION

This study reports a comprehensive characterization of the coding genome of tFL, an aggressive disease with dismal prognosis, the pathogenesis of which has been incompletely understood so far. Our goal was to take advantage of systematic, genome-wide approaches in order to address key questions related to this aggressive condition that have remained unanswered or had been previously only studied by examining individual genes. These include: (1) tracing the evolutionary history of the dominant clone during transformation from indolent FL, (2) providing an assessment of the range and frequency of genetic aberrations that are associated with this event, (3) identifying genomic changes as potential genetic drivers of transformation, and (4) elucidating the relationship between DLBCL deriving from FL transformation and DLBCL arising de novo.

The first finding of our study is that, although all FL-tFL sample pairs have a clear clonal relationship, the dominant tFL clone arises in most patients from a mutated CPC through the acquisition of independent genetic events, consistent with divergent evolution. The existence of this CPC cannot be physically demonstrated, but it can be postulated on the basis of the presence of a set of lesions that are shared between FL and tFL, and is consistent with previous studies based on the analysis of the rearranged Ig genes (Carlotti et al., 2009) as well as with recent work on FL progression (Green et al., 2013). Our study does not address the topography of the tFL clone and/or the intraclonal architecture of these tumors, which require the backtracking of tFL-specific lesions in the diagnostic FL sample by ultrahigh deep sequencing analysis (Ding et al., 2012; Walter et al., 2012; Welch et al., 2012). Thus, additional studies will be needed in order to clarify whether the tFL clone temporally developed after FL diagnosis or whether it can be already detected as a minor subclone within the FL diagnostic sample. Notably, the two most prominent programs deregulated in the precursor clone—epigenetic modifications and resistance to apoptosis—represent actionable targets, and a number of drugs are already being tested in the clinic (e.g., BCL2 inhibitors, histone deacetylase inhibitors, and EZH2 inhibitors) (Sawas et al., 2011). If these lesions are essential to the survival of the fully transformed tumor cells and if the tFL clone is not already present at FL diagnosis, then the development of combination regimens incorporating drugs that specifically target this group of alterations in early stages of FL may lead to the elimination of the precursor clone, possibly preventing transformation.

Our study reveals that, although the genome of tFL is significantly more complex in comparison to FL, no unifying genetic lesion is selected during transformation to DLBCL. Nonetheless, the recurrent alteration of genes involved in the control of cell-cycle progression (*CDKN2A/B* and *MYC*) and DNA damage responses (alternative biallelic loss of *TP53* and *CDKN2A*) suggest that a loss of genetic stability and deregulated proliferation are critical steps in tFL development. Lesions affecting *CDKN2A/B* have been observed in several terminally aggressive lymphoid malignancies, including relapsed acute lymphoblastic leukemia (Mullighan et al., 2008), Richter syndrome (Fabbri et al., 2013), and ABC-DLBCL (Lenz et al., 2008), consistent with a central role in the acquisition of a more aggressive phenotype. The existence of tFL cases that lack p16 expression despite being devoid of *CDKN2A* genetic lesions suggests an even broader

involvement of this pathway through alternative epigenetic mechanisms (e.g., promoter hypermethylation or posttranscriptional modifications). Furthermore, the inactivation of epigenetic modifiers such as CREBBP/EP300 and MLL2 may also contribute to the deregulation of cell growth and DNA damage responses by interfering with p53 acetylation and activation (Pasqualucci et al., 2011a).

The genomic complexity of tFL appears to be remarkably high in respect to other hematologic malignancies, as exemplified by the presence of numerous CNAs and the evidence of ASHM. The latter may represent a major mechanism for transformation, as previously suggested for de novo DLBCL (Pasqualucci et al., 2001). Interestingly, although the physiologic SHM process is known to operate in FL (Bahler and Levy, 1992), ASHM was only observed in the dominant clone of tFL, pointing to a disruption occurring late during evolution to or selection of a more aggressive disease. Although the analysis presented here did not uncover any apparent lesions in genes that are directly involved in SHM, the alteration of histone marks owing to genetic lesions in histone modification and chromatin remodeling enzymes may induce chromatin conformation changes that favor the accessibility of nonphysiologic genomic target regions to the AID mutator. Thus, additional studies interrogating the entire genome as well as the epigenome of this cancer will be necessary in order to conclusively address this question.

Finally, and consistent with observations obtained by gene expression profiling, our data highlight tFL as a distinct disease that, although more similar to GCB-DLBCL, harbors unique combinations of oncogenic and tumor suppressor lesions in comparison to de novo DLBCL. Previous studies have suggested that transformation proceeds through two distinct pathways: one characterized by a high-proliferation signature, and a second where T cell and follicular dendritic-associated genes predominate (Davies et al., 2007; Lossos et al., 2002). We did not observe statistically significant mutual exclusion between genetic lesions affecting these two classes of mutated genes (e.g., *MYC* and *CDKN2A/B* versus *TNFRSF14* and *STAT6*). However, integrated genomic and transcriptional profiling of larger cohorts of patients will be needed in order to address this question. The unique tFL genomic landscape, combining alterations that are specific to GCB- and ABC-DLBCL as well as lesions that are uncommon in de novo DLBCL, could be responsible, at least in part, for its poor response to standard anti-DLBCL regimens. The results herein suggest the potential usefulness of combining current immunochemotherapeutic regimens that harness the proliferative and genetically unstable phenotype of tFL with more specific approaches targeting some of the pathways recurrently altered in tFL, as it could be the case for CDK4/6 activation deriving from the loss of *CDKN2A* or NF-κB activation deriving from *TNFAIP3* deletions and/or mutations.

EXPERIMENTAL PROCEDURES

Study Panel

A discovery panel of 24 sequential fresh-frozen biopsies (12 pairs) obtained at FL diagnosis and at transformation to DLBCL (Table S1) and a screening panel of 27 tFL samples were selected on the basis of the criteria described in the Supplemental Information, and were used for WES and SNP6.0 array analysis. Matched normal DNA was available for 4 of the 12 discovery pairs and was documented to lack contaminating tumor cells by PCR amplification of the clonally rearranged tumor-associated Ig genes as well as by SNP array analysis of the corresponding loci. Using these 12 pairs, we estimate a 99% probability of detecting mutations that affect genes at 30% prevalence and 93% probability for genes at 20% prevalence.

Whole-Exome Capture and Next-Generation Sequencing

Purified high-molecular-weight genomic DNA (~3 μg) from the 12 FL and 39 tFL samples (n = 12 from the discovery panel and 27 from the screening panel) was enriched in protein-coding sequences with the Agilent SureSelect Human 51Mb All Exon v4 Kit (Agilent Technologies) according to the manufacturer's protocol. The resulting target-enriched pool was normalized and combined (four-plex) before high-throughput paired-end (2 × 100 bp) sequencing was performed on the Illumina HiSeq2000 System at Centrillion Biosciences. The analysis produced on average 67.5 million passed-filter paired-end reads per sample (range, 51.7 to 111.6; Table S2). After filtering for duplicate reads (defined as reads with identical start and orientation), sequences were aligned to the reference human genome hg19 assembly (GRCh37) with the Burrows-Wheeler Aligner tool (version 0.5.9). The mean coverage depth (i.e., the mean number of reads covering the target exome of a haploid reference) was 80.8× (range, 45.8 to 119.4) with an average of 89.3% of the captured region covered at >10× (range, 83.8 to 93.4) and 73.9% covered at >30× (range, 53.9 to 84.5; Table S2). Sequence variants, including nucleotide substitutions and small insertions and/or deletions, were obtained independently for each tumor and normal sample with the Statistical Algorithm for Variant Identification (Trifonov et al., 2013b) and were independently validated by conventional Sanger sequencing, as described in the Supplemental Experimental Procedures.

Dominant Clone Analysis

For the purpose of reconstructing the history of clonal evolution during FL transformation to DLBCL, we first estimated the percentage of tumor cells in the biopsy on the basis of the inferred CN value at the clonally rearranged Ig loci (i.e., the region of intrachromosomal deletional recombination at 14q32, 2p11, and 11q22). Then, the allelic frequency of each SNV was corrected for the fraction of tumor cells in the biopsy by calculating its expected frequency, the 95% CIs from its observed frequency, the total depth at the variant position, and the tumor content of the sample, assuming a binomial distribution.

Mutations were classified as clonal if the fraction of variant reads (upon correction for the percentage of tumor cells in the specimen) was > 20 and were classified as subclonal otherwise. Because this analysis focuses on the history of the dominant tumor clone, only SNVs that were clonally represented in at least one disease phase were considered. Then, SNVs were assigned to one of the following three categories: (1) shared mutations (i.e., mutations that are detected in the major clone of both diseases phases), (2) FL-specific mutations (i.e., mutations present in the major clone of the FL phase and either completely absent or present at subclonal levels in the paired tFL specimen, provided the difference in the corrected frequencies between the two phases was statistically significant at $p < 0.05$ [as explained below] and after excluding that its absence in the paired tFL specimen was not due to CN loss or cnLOH involving the same genomic region), and (3) tFL-specific mutations (i.e., mutations present in the major clone of the tFL phase and absent or subclonal in the FL biopsy provided the difference in the corrected frequencies between the two phases was statistically significant at $p < 0.05$ and could not be explained by CN loss or cnLOH in the latter). To assess whether the difference in frequencies between the two phases was significant, we considered a binomial distribution and calculated the probability of observing the variant in the pretransformation (or posttransformation) phase, given the coverage depth at that position, the observed frequency of variant reads in the paired sample, and the estimated tumor content of the samples. WES and SNP6.0 analysis were used to exclude that the absence of FL-specific SNVs in the longitudinal tFL biopsy was due to recombination events, such as CN losses or cnLOH affecting the same region; the few mutations belonging to this category were conservatively classified as "shared" (in cases with paired normal DNA) or were excluded (in cases without paired normal DNA). Mutations that were

clonally represented in the tFL phase but could be detected in a small fraction of reads in the FL phase (with $p < 0.05$) were defined as DLBCL-specific, given that they most likely reflect a pre-existing smaller clone within the FL major clone, whereas mutations that were clonally represented in the FL phase but were also detected in a small fraction of the tFL population (with $p < 0.05$) were considered as FL-specific, given that they may reflect residual FL cells amidst the DLBCL clone, which were not selected during progression and expansion.

High-Density SNP Array Analysis, Sequencing Analysis of ASHM Target Genes, FISH, and Immunohistochemistry Analysis

High-density SNP array analysis, sequencing analysis of ASHM target genes, FISH, and immunohistochemistry analysis were all performed as previously described, and their detailed protocols can be found in the Supplemental Information.

ACCESSION NUMBERS

The Affymetrix SNP Array 6.0 data and the whole-exome sequencing data from the 12 FL and 39 tFL cases have been deposited in NCBI database of Genotypes and Phenotypes under accession number phs000328.v2.p1.

SUPPLEMENTAL INFORMATION

Supplemental Information contains Supplemental Experimental Procedures, seven figures, and seven tables and can be found with this article online at http://dx.doi.org/10.1016/j.celrep.2013.12.027.

ACKNOWLEDGMENTS

We thank G. Fabbri for discussions, V. Miljkovic for help with the SNP array hybridization, and the Molecular Pathology Shared Resource and the Molecular Cytogenetics and Epigenetics Shared Resource of the Herbert Irving Comprehensive Cancer Center at Columbia University for histology service and cytogenetics service, respectively. We also thank R. Feldman and R. Mei for expert assistance with the whole-exome capture and sequencing, which were completed at Centrillion Biosciences. Automated DNA sequencing was performed at GENEWIZ. This work was supported by the NIH (RO1-CA37295 to R.D.-F., RO1-CA172492-01 to L.P., and RO1-CA136537 to S.N.M.), a Specialized Center of Research grant from the Leukemia & Lymphoma Society (to R.D.-F.), the Northeast Biodefense Center (U54-AI057158), and the National Library of Medicine (1R01LM010140-01 to R.R.), the AIRC Special Program Molecular Clinical Oncology – 5 per mille (contract 10007 to G.G. and G.I.), and the Cariplo Foundation (to G.G.). L.P. is on leave from the Institute of Hematology, University of Perugia Medical School. M.F. was enrolled in the PhD program in Clinical and Experimental Medicine at Amedeo Avogadro University of Eastern Piedmont and was supported in part by the Novara AIL.

Received: August 11, 2013
Revised: November 27, 2013
Accepted: December 16, 2013
Published: January 2, 2014

REFERENCES

Akasaka, T., Lossos, I.S., and Levy, R. (2003). BCL6 gene translocation in follicular lymphoma: a harbinger of eventual transformation to diffuse aggressive lymphoma. Blood *102*, 1443–1448.

Alizadeh, A.A., Eisen, M.B., Davis, R.E., Ma, C., Lossos, I.S., Rosenwald, A., Boldrick, J.C., Sabet, H., Tran, T., Yu, X., et al. (2000). Distinct types of diffuse large B-cell lymphoma identified by gene expression profiling. Nature *403*, 503–511.

Bahler, D.W., and Levy, R. (1992). Clonal evolution of a follicular lymphoma: evidence for antigen selection. Proc. Natl. Acad. Sci. USA *89*, 6770–6774.

Bergsagel, P.L., and Kuehl, W.M. (2013). Degree of focal immunoglobulin heavy chain locus deletion as a measure of B-cell tumor purity. Leukemia *27*, 2067–2068.

Carlotti, E., Wrench, D., Matthews, J., Iqbal, S., Davies, A., Norton, A., Hart, J., Lai, R., Montoto, S., Gribben, J.G., et al. (2009). Transformation of follicular lymphoma to diffuse large B-cell lymphoma may occur by divergent evolution from a common progenitor cell or by direct evolution from the follicular lymphoma clone. Blood *113*, 3553–3557.

Challa-Malladi, M., Lieu, Y.K., Califano, O., Holmes, A.B., Bhagat, G., Murty, V.V., Dominguez-Sola, D., Pasqualucci, L., and Dalla-Favera, R. (2011). Combined genetic inactivation of β2-Microglobulin and CD58 reveals frequent escape from immune recognition in diffuse large B cell lymphoma. Cancer Cell *20*, 728–740.

Davies, A.J., Rosenwald, A., Wright, G., Lee, A., Last, K.W., Weisenburger, D.D., Chan, W.C., Delabie, J., Braziel, R.M., Campo, E., et al. (2007). Transformation of follicular lymphoma to diffuse large B-cell lymphoma proceeds by distinct oncogenic mechanisms. Br. J. Haematol. *136*, 286–293.

Ding, L., Ley, T.J., Larson, D.E., Miller, C.A., Koboldt, D.C., Welch, J.S., Ritchey, J.K., Young, M.A., Lamprecht, T., McLellan, M.D., et al. (2012). Clonal evolution in relapsed acute myeloid leukaemia revealed by whole-genome sequencing. Nature *481*, 506–510.

Fabbri, G., Rasi, S., Rossi, D., Trifonov, V., Khiabanian, H., Ma, J., Grunn, A., Fangazio, M., Capello, D., Monti, S., et al. (2011). Analysis of the chronic lymphocytic leukemia coding genome: role of NOTCH1 mutational activation. J. Exp. Med. *208*, 1389–1401.

Fabbri, G., Khiabanian, H., Holmes, A.B., Wang, J., Messina, M., Mullighan, C.G., Pasqualucci, L., Rabadan, R., and Dalla-Favera, R. (2013). Genetic lesions associated with chronic lymphocytic leukemia transformation to Richter syndrome. J. Exp. Med. *210*, 2273–2288.

Green, M.R., Gentles, A.J., Nair, R.V., Irish, J.M., Kihira, S., Liu, C.L., Kela, I., Hopmans, E.S., Myklebust, J.H., Ji, H., et al. (2013). Hierarchy in somatic mutations arising during genomic evolution and progression of follicular lymphoma. Blood *121*, 1604–1611.

Ho, L., Ronan, J.L., Wu, J., Staahl, B.T., Chen, L., Kuo, A., Lessard, J., Nesvizhskii, A.I., Ranish, J., and Crabtree, G.R. (2009). An embryonic stem cell chromatin remodeling complex, esBAF, is essential for embryonic stem cell self-renewal and pluripotency. Proc. Natl. Acad. Sci. USA *106*, 5181–5186.

Holzelova, E., Vonarbourg, C., Stolzenberg, M.C., Arkwright, P.D., Selz, F., Prieur, A.M., Blanche, S., Bartunkova, J., Vilmer, E., Fischer, A., et al. (2004). Autoimmune lymphoproliferative syndrome with somatic Fas mutations. N. Engl. J. Med. *351*, 1409–1418.

Korbel, J.O., and Campbell, P.J. (2013). Criteria for inference of chromothripsis in cancer genomes. Cell *152*, 1226–1236.

Kridel, R., Sehn, L.H., and Gascoyne, R.D. (2012). Pathogenesis of follicular lymphoma. J. Clin. Invest. *122*, 3424–3431.

Lawrence, M.S., Stojanov, P., Polak, P., Kryukov, G.V., Cibulskis, K., Sivachenko, A., Carter, S.L., Stewart, C., Mermel, C.H., Roberts, S.A., et al. (2013). Mutational heterogeneity in cancer and the search for new cancer-associated genes. Nature *499*, 214–218.

Lenz, G., Wright, G.W., Emre, N.C., Kohlhammer, H., Dave, S.S., Davis, R.E., Carty, S., Lam, L.T., Shaffer, A.L., Xiao, W., et al. (2008). Molecular subtypes of diffuse large B-cell lymphoma arise by distinct genetic pathways. Proc. Natl. Acad. Sci. USA *105*, 13520–13525.

Lo Coco, F., Gaidano, G., Louie, D.C., Offit, K., Chaganti, R.S., and Dalla-Favera, R. (1993). p53 mutations are associated with histologic transformation of follicular lymphoma. Blood *82*, 2289–2295.

Lohr, J.G., Stojanov, P., Lawrence, M.S., Auclair, D., Chapuy, B., Sougnez, C., Cruz-Gordillo, P., Knoechel, B., Asmann, Y.W., Slager, S.L., et al. (2012). Discovery and prioritization of somatic mutations in diffuse large B-cell lymphoma (DLBCL) by whole-exome sequencing. Proc. Natl. Acad. Sci. USA *109*, 3879–3884.

Lossos, I.S., and Gascoyne, R.D. (2011). Transformation of follicular lymphoma. Best Pract. Res. Clin. Haematol. *24*, 147–163.

Lossos, I.S., Alizadeh, A.A., Diehn, M., Warnke, R., Thorstenson, Y., Oefner, P.J., Brown, P.O., Botstein, D., and Levy, R. (2002). Transformation of follicular lymphoma to diffuse large-cell lymphoma: alternative patterns with increased or decreased expression of c-myc and its regulated genes. Proc. Natl. Acad. Sci. USA *99*, 8886–8891.

Mandelbaum, J., Bhagat, G., Tang, H., Mo, T., Brahmachary, M., Shen, Q., Chadburn, A., Rajewsky, K., Tarakhovsky, A., Pasqualucci, L., and Dalla-Favera, R. (2010). BLIMP1 is a tumor suppressor gene frequently disrupted in activated B cell-like diffuse large B cell lymphoma. Cancer Cell *18*, 568–579.

Martinez-Climent, J.A., Alizadeh, A.A., Segraves, R., Blesa, D., Rubio-Moscardo, F., Albertson, D.G., Garcia-Conde, J., Dyer, M.J., Levy, R., Pinkel, D., and Lossos, I.S. (2003). Transformation of follicular lymphoma to diffuse large cell lymphoma is associated with a heterogeneous set of DNA copy number and gene expression alterations. Blood *101*, 3109–3117.

Montoto, S., and Fitzgibbon, J. (2011). Transformation of indolent B-cell lymphomas. J. Clin. Oncol. *29*, 1827–1834.

Morin, R.D., Johnson, N.A., Severson, T.M., Mungall, A.J., An, J., Goya, R., Paul, J.E., Boyle, M., Woolcock, B.W., Kuchenbauer, F., et al. (2010). Somatic mutations altering EZH2 (Tyr641) in follicular and diffuse large B-cell lymphomas of germinal-center origin. Nat. Genet. *42*, 181–185.

Morin, R.D., Mendez-Lago, M., Mungall, A.J., Goya, R., Mungall, K.L., Corbett, R.D., Johnson, N.A., Severson, T.M., Chiu, R., Field, M., et al. (2011). Frequent mutation of histone-modifying genes in non-Hodgkin lymphoma. Nature *476*, 298–303.

Morin, R.D., Mungall, K., Pleasance, E., Mungall, A.J., Goya, R., Huff, R.D., Scott, D.W., Ding, J., Roth, A., Chiu, R., et al. (2013). Mutational and structural analysis of diffuse large B-cell lymphoma using whole-genome sequencing. Blood *122*, 1256–1265.

Mullighan, C.G., Goorha, S., Radtke, I., Miller, C.B., Coustan-Smith, E., Dalton, J.D., Girtman, K., Mathew, S., Ma, J., Pounds, S.B., et al. (2007). Genome-wide analysis of genetic alterations in acute lymphoblastic leukaemia. Nature *446*, 758–764.

Mullighan, C.G., Phillips, L.A., Su, X., Ma, J., Miller, C.B., Shurtleff, S.A., and Downing, J.R. (2008). Genomic analysis of the clonal origins of relapsed acute lymphoblastic leukemia. Science *322*, 1377–1380.

Ngo, V.N., Young, R.M., Schmitz, R., Jhavar, S., Xiao, W., Lim, K.H., Kohlhammer, H., Xu, W., Yang, Y., Zhao, H., et al. (2011). Oncogenically active MYD88 mutations in human lymphoma. Nature *470*, 115–119.

Pasqualucci, L., Neumeister, P., Goossens, T., Nanjangud, G., Chaganti, R.S., Küppers, R., and Dalla-Favera, R. (2001). Hypermutation of multiple proto-oncogenes in B-cell diffuse large-cell lymphomas. Nature *412*, 341–346.

Pasqualucci, L., Compagno, M., Houldsworth, J., Monti, S., Grunn, A., Nandula, S.V., Aster, J.C., Murty, V.V., Shipp, M.A., and Dalla-Favera, R. (2006). Inactivation of the PRDM1/BLIMP1 gene in diffuse large B cell lymphoma. J. Exp. Med. *203*, 311–317.

Pasqualucci, L., Dominguez-Sola, D., Chiarenza, A., Fabbri, G., Grunn, A., Trifonov, V., Kasper, L.H., Lerach, S., Tang, H., Ma, J., et al. (2011a). Inactivating mutations of acetyltransferase genes in B-cell lymphoma. Nature *471*, 189–195.

Pasqualucci, L., Trifonov, V., Fabbri, G., Ma, J., Rossi, D., Chiarenza, A., Wells, V.A., Grunn, A., Messina, M., Elliot, O., et al. (2011b). Analysis of the coding genome of diffuse large B-cell lymphoma. Nat. Genet. *43*, 830–837.

Pinyol, M., Cobo, F., Bea, S., Jares, P., Nayach, I., Fernandez, P.L., Montserrat, E., Cardesa, A., and Campo, E. (1998). p16(INK4a) gene inactivation by deletions, mutations, and hypermethylation is associated with transformed and aggressive variants of non-Hodgkin's lymphomas. Blood *91*, 2977–2984.

Ritz, O., Guiter, C., Castellano, F., Dorsch, K., Melzner, J., Jais, J.P., Dubois, G., Gaulard, P., Möller, P., and Leroy, K. (2009). Recurrent mutations of the STAT6 DNA binding domain in primary mediastinal B-cell lymphoma. Blood *114*, 1236–1242.

Rossi, D., Berra, E., Cerri, M., Deambrogi, C., Barbieri, C., Franceschetti, S., Lunghi, M., Conconi, A., Paulli, M., Matolcsy, A., et al. (2006). Aberrant somatic hypermutation in transformation of follicular lymphoma and chronic lymphocytic leukemia to diffuse large B-cell lymphoma. Haematologica *91*, 1405–1409.

Rossi, D., Trifonov, V., Fangazio, M., Bruscaggin, A., Rasi, S., Spina, V., Monti, S., Vaisitti, T., Arruga, F., Famà, R., et al. (2012). The coding genome of splenic marginal zone lymphoma: activation of NOTCH2 and other pathways regulating marginal zone development. J. Exp. Med. *209*, 1537–1551.

Saito, M., Novak, U., Piovan, E., Basso, K., Sumazin, P., Schneider, C., Crespo, M., Shen, Q., Bhagat, G., Califano, A., et al. (2009). BCL6 suppression of BCL2 via Miz1 and its disruption in diffuse large B cell lymphoma. Proc. Natl. Acad. Sci. USA *106*, 11294–11299.

Sander, C.A., Yano, T., Clark, H.M., Harris, C., Longo, D.L., Jaffe, E.S., and Raffeld, M. (1993). p53 mutation is associated with progression in follicular lymphomas. Blood *82*, 1994–2004.

Sawas, A., Diefenbach, C., and O'Connor, O.A. (2011). New therapeutic targets and drugs in non-Hodgkin's lymphoma. Curr. Opin. Hematol. *18*, 280–287.

Sherr, C.J. (2004). Principles of tumor suppression. Cell *116*, 235–246.

Siegel, R.M., Frederiksen, J.K., Zacharias, D.A., Chan, F.K., Johnson, M., Lynch, D., Tsien, R.Y., and Lenardo, M.J. (2000). Fas preassociation required for apoptosis signaling and dominant inhibition by pathogenic mutations. Science *288*, 2354–2357.

Swerdlow, S.H., Campo, E., Harris, N.L., Jaffe, E.S., Pileri, S.A., Stein, H., Thiele, J., and Vardiman, J.W. (2008). WHO Classification of Tumours of Haematopoietic and Lymphoid Tissues. International Agency for Research on Cancer (Geneva: World Health Organization).

Trifonov, V., Pasqualucci, L., Dalla Favera, R., and Rabadan, R. (2013a). MutComFocal: an integrative approach to identifying recurrent and focal genomic alterations in tumor samples. BMC Syst. Biol. *7*, 25.

Trifonov, V., Pasqualucci, L., Tiacci, E., Falini, B., and Rabadan, R. (2013b). SAVI: a statistical algorithm for variant frequency identification. BMC Syst. Biol. *7* (*Suppl 2*), S2.

Trinh, D.L., Scott, D.W., Morin, R.D., Mendez-Lago, M., An, J., Jones, S.J., Mungall, A.J., Zhao, Y., Schein, J., Steidl, C., et al. (2013). Analysis of FOXO1 mutations in diffuse large B-cell lymphoma. Blood *121*, 3666–3674.

van Eijk, M., Defrance, T., Hennino, A., and de Groot, C. (2001). Death-receptor contribution to the germinal-center reaction. Trends Immunol. *22*, 677–682.

Walter, M.J., Shen, D., Ding, L., Shao, J., Koboldt, D.C., Chen, K., Larson, D.E., McLellan, M.D., Dooling, D., Abbott, R., et al. (2012). Clonal architecture of secondary acute myeloid leukemia. N. Engl. J. Med. *366*, 1090–1098.

Welch, J.S., Ley, T.J., Link, D.C., Miller, C.A., Larson, D.E., Koboldt, D.C., Wartman, L.D., Lamprecht, T.L., Liu, F., Xia, J., et al. (2012). The origin and evolution of mutations in acute myeloid leukemia. Cell *150*, 264–278.